HHS Public Access

Author manuscript

J Am Soc Mass Spectrom. Author manuscript; available in PMC 2016 June 01.

Published in final edited form as:

J Am Soc Mass Spectrom. 2015 June ; 26(6): 924–933. doi:10.1007/s13361-015-1131-0.

Profiling and Imaging Ion Mobility-Mass Spectrometry Analysis of Cholesterol and 7-Dehydrocholesterol in Cells Via Sputtered Silver MALDI

Libin Xu[1,2,6], **Michal Kliman**[1,2,3,7], **Jay G. Forsythe**[1,2,3,8], **Zeljka Korade**[4], **Anthony B. Hmelo**[5], **Ned A. Porter**[1,2], and **John A. McLean**[1,2,3]

[1]Department of Chemistry, Vanderbilt University, Nashville, TN 37235, USA

[2]Vanderbilt Institute of Chemical Biology, Vanderbilt University, Nashville, TN 37235, USA

[3]Vanderbilt Institute for Integrative Biosystems Research and Education, Vanderbilt University, Nashville, TN 37235, USA

[4]Department of Psychiatry and Vanderbilt Kennedy Center for Research on Human Development, Vanderbilt University, Nashville, TN 37235, USA

[5]Department of Physics and Astronomy, Vanderbilt University, Nashville, TN 37235, USA

[6]*Present Address:* Department of Medicinal Chemistry, University of Washington, Seattle, WA, USA

[7]*Present Address:* Allergan, Inc., Irvine, CA, USA

[8]*Present Address:* School of Chemistry and Biochemistry, Georgia Institute of Technology, Atlanta, GA, USA

Abstract

Profiling and imaging of cholesterol and its precursors by mass spectrometry (MS) are important in a number of cholesterol biosynthesis disorders, such as in Smith-Lemli-Opitz syndrome (SLOS), where 7-dehydrocholesterol (7-DHC) is accumulated in affected individuals. SLOS is caused by defects in the enzyme that reduces 7-DHC to cholesterol. However, analysis of sterols is challenging because these hydrophobic olefins are difficult to ionize for MS detection. We report here sputtered silver matrix-assisted laser desorption/ionization (MALDI)-ion mobility-MS (IM-MS) analysis of cholesterol and 7-DHC. In comparison with liquid-based $AgNO^3$ and colloidal Ag nanoparticle (AgNP), sputtered silver NP (10–25 nm) provided the lowest limits-of-detection based on the silver coordinated $[cholesterol+Ag]^+$ and $[7\text{-}DHC+Ag]^+$ signals while minimizing dehydrogenation products ($[M+Ag-2H]^+$). When analyzing human fibroblasts that were directly grown on poly-L-lysine-coated ITO glass plates with this technique, in situ, the 7-DHC/cholesterol ratios for both control and SLOS human fibroblasts are readily obtained. The *m/z* of 491 (specific for $[7\text{-}DHC+^{107}Ag]^+$) and 495 (specific for $[cholesterol+^{109}Ag]^+$) were subsequently

Correspondence to: John A. McLean; john.a.mclean@vanderbilt.edu.
Libin Xu and Michal Kliman contributed equally to this work.

Electronic supplementary material The online version of this article (doi:10.1007/s13361-015-1131-0) contains supplementary material, which is available to authorized users.

imaged using MALDI-IM-MS. MS images were co-registered with optical images of the cells for metabolic ratio determination. From these comparisons, ratios of 7-DHC/cholesterol for SLOS human fibroblasts are distinctly higher than in control human fibroblasts. Thus, this strategy demonstrates the utility for diagnosing/assaying the severity of cholesterol biosynthesis disorders in vitro.

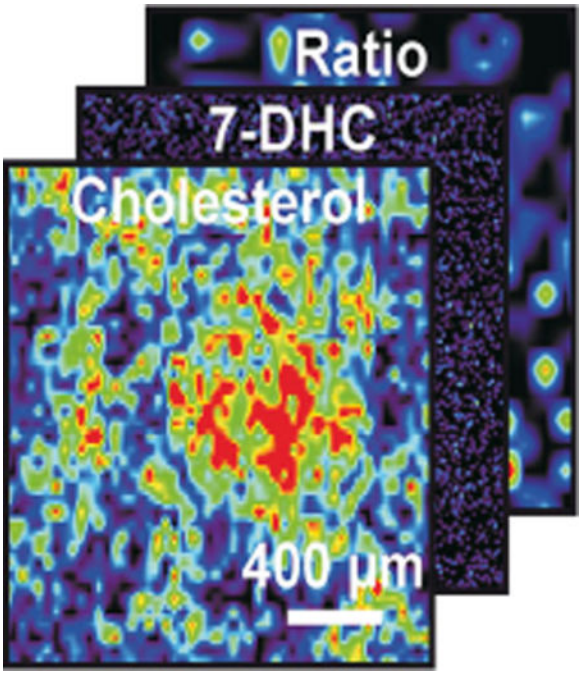

Keywords

Sputter coating; Silver; Cholesterol; 7-Dehydrocholesterol; Ion mobility-mass spectrometry; Imaging; Smith-Lemli-Opitz syndrome

Introduction

Cholesterol is a major component of the cell membrane and plays important structural and functional roles in biological processes. For example, cholesterol is abundant in lipid rafts, membrane microdomains that serve as important media in cell signaling [1, 2]. In addition, cholesterol constitutes ca. 20% of total lipids in the brain and is essential in activating the hedgehog signaling pathway that is critical for embryonic development [3, 4]. A number of defects in cholesterol biosynthesis lead to elevated levels of sterol precursors, such as in Smith-Lemli-Opitz syndrome (SLOS), where 7-dehydrocholesterol (7-DHC) accumulates in affected individuals because of defective 3β-hydroxysterol-Δ^7-reductase (DHCR7) [5]. In addition, abnormal levels of cholesterol or its precursors/metabolites have been observed in various human diseases, such as atherosclerosis [6], Niemann-Pick C1 diseases [7], cerebrotendinous xanthomatosis [8], breast cancer [9], etc. Thus, it is critical to assay and/or image cholesterol and related sterols from cells, tissues, or fluids in situ to quickly diagnose related diseases and to understand the distribution of cholesterol and its precursors.

Hydrophobic olefins, including cholesterol and related sterols, steroids, and some vitamins, are difficult to ionize for subsequent mass spectrometry (MS) analysis. For this reason, silver has been used to ionize such molecules in coordination ion-spray MS (CIS-MS), taking advantage of the electrophilic nature of silver to coordinate directly with unsaturated carbon–carbon bonds [10, 11]. Typically, doublet peaks of the analyte-silver adducts, $[M+^{107}Ag]^+$ and $[M+^{109}Ag]^+$, are observed because of the similar relative abundance of the two stable isotopes of silver. Direct laser desorption/ionization (LDI) of $[cholesterol+Ag]^+$ complexes was achieved in a mixture of peptides and phospholipids [12], and in astrocyte cells with the assistance of silver nanoparticles (AgNPs) [13]. The sensitivity of this technique was further improved by the application of monoisotopic AgNPs by restricting ion species to a single silver isotope [14]. More recently, direct silver coating in the form of aqueous $AgNO_3$, coupled with nanostructure-initiator-MS (NIMS), was used to image cholesterol and 7-DHC from brain tissues in a SLOS mouse model [15]. All of these methods required liquid-based sample preparation, which can result in analyte diffusion from their native locations in tissues or cells. Clearly, this is undesirable when performing MS imaging experiments at high spatial resolution because resolution is then limited by the competing kinetics of solvent evaporation and diffusion, rather than the instrumental methodologies for imaging MS. In contrast with liquid-based techniques, gas-based sputter deposition is a fast and reproducible way to generate AgNPs directly on surfaces without solvent. In gas-phase sputter deposition, particle sizes and film thicknesses can be controlled by varying the applied voltage, sputtering time, inert gas pressure, and distance from the sputtering target [16]. Moreover, sputter coating samples with metal increases the conductivity of insulating substrates, such as tissues or cells, which is believed to increase ion signal and mitigate surface charging aberrations in imaging MS [17]. The ionization of cholesterol in cells and/or tissues using sputtered silver was demonstrated previously for secondary ionization-MS (SIMS) detection and more recently for LDI-MS [18–22]. Although SIMS has the advantage of generating MS images with high spatial resolution, it tends to produce more fragment ions than LDI-MS methods [18, 21].

The present research centers on the utility of sputtered silver for imaging IM-MS of cells grown directly on glass sample targets for the quantitation of cholesterol and cholesterol metabolic precursors. There are compelling motivations to describe the workflow utilized here as either direct LDI or matrix-assisted LDI (MALDI). We are inclined to describe the sputtered silver deposition as MALDI because the AgNP serves as both a chromophore for UV irradiation and as a source of cationizing species (i.e., Ag^+) to facilitate ionization of the analyte. Note that the AgNP utilized in this work are in a similar size range to the 30 nm cobalt particles used by Tanaka and coworkers in their seminal MALDI demonstration [23], and the MALDI terminology has also been used to describe the utility of AuNP as MALDI matrices [24].

Here we report: (1) a critical comparison of liquid-based versus gas-based silver deposition for MALDI-IM-MS analysis of cholesterol and 7-DHC, (2) a MALDI-IM-MS quantitation strategy for cholesterol and 7-DHC from human fibroblast cells through silver complexation, and (3) direct imaging MALDI-IM-MS of cholesterol and 7-DHC from monolayers of control and SLOS human fibroblast cells that were grown directly on ITO-coated glass plates.

Experimental

Materials

Cholesterol, 7-DHC, $AgNO_3$, poly-L-lysine, and acetonitrile were purchased from Sigma-Aldrich Co. ITO-coated float glass MALDI plates (part no. CG-90IN-3081; 70–100 Ω; 45×45×1.1 mm) were purchased from Delta Technologies, Ltd. (Loveland, CO, USA). Colloidal AgNP (nominal particle size: 20 nm; particle concentration: 0.12 nM; Ag concentration 28.5 μM) was purchased from Ted Pella, Inc. (Redding, CA, USA).

Ion Mobility-Mass Spectrometry

All data were acquired on a MALDI-IM-MS (Synapt G2 HDMS; Waters Corp., Milford, MA, USA) using a frequency-tripled Nd:YAG laser (wavelength=355 nm, pulse repetition frequency=1000.0 Hz). Data were acquired in Resolution mode and, unless otherwise indicated in selected measurements, over a mass range of 400 to 600*m/z* for sterol standards in characterization and development of the technique and a mass range of 480 to 510*m/z* for imaging-mode acquisition. Laser energy attenuation was 300 (arbitrary units) for cholesterol and 7-DHC standards and 250 for ionization directly from cells. Ion mobility separation was performed at a drift gas pressure of 2.30 Torr using nitrogen gas, a wave velocity of 650 m/s, and a wave height of 40.0 V.

Gas-Based and Liquid-Based Silver Deposition Strategies

Stock solutions of cholesterol and 7-DHC (1.55 and 1.43 mM, respectively) were prepared in acetonitrile, and 0.5 μL of stock solutions were spotted on an ITO-coated glass plate in triplicates (resulting in spots of ca. 2 mm^2 area with 390 pmol/mm^2 of cholesterol or 360 pmol/mm^2 of 7-DHC). Sputter coating was performed with a Cressington Sputter Coater 108 (Ted Pella, Inc., Redding, CA, USA) at a current of 30 mA and an atmosphere of 0.15 Torr of Ar over different durations (100, 300, 600, 900, 1200, 1500 s). The distance between silver target and the sample plate being coated was set at 8 cm. The samples were analyzed by MALDI-IM-MS and comparison of spectra suggested that 600 s of coating gave the highest signal intensity. Using these sputter conditions, the limits of detection for cholesterol and 7-DHC standards were obtained. To account for differences in ionization efficiency in metabolic ratio calculations, a response factor for 7-DHC relative to cholesterol was obtained by co-spotting known amounts of 7-DHC and cholesterol followed by sputter coating. For liquid-based silver deposition, different quantities of either $AgNO_3$ (23, 230, and 2300 pmol) or AgNP (0.06, 0.12, 0.18 fmol of NP or 14.3, 28.6, and 42.9 pmol of Ag) were spotted on top of the sample spots (390 pmol/mm^2 of cholesterol or 360 pmol/mm^2 of 7-DHC), dried under vacuum, and subsequently analyzed by MALDI-IM-MS.

Cell Culture for Determining Limits of Detection

Control (GM05399) and SLOS (GM05788) human fibroblasts were purchased from the Coriell Institute (Camden, NJ, USA). Both cell lines were grown in Dulbecco's modified eagle medium (DMEM) supplemented with L-glutamine, 10% lipid-reduced fetal bovine serum (FBS; Thermo Scientific HyClone, Logan, UT, USA), and penicillin/streptomycin at 37°C and 5% CO_2, for 6 d as described previously [25]. The cells were trypsinized, counted,

and resuspended in 1× PBS/H_2O (1/1) at different concentrations. Approximately 2 μL of each cell suspension was manually spotted on ITO-coated glass plates, resulting in a spot area of ca. 2 mm^2. Each cell concentration was spotted in triplicate, where reproducibility was found to be high as indicated in the data below for determination of limits of detection. Final concentrations of 100, 1000, and 10,000 cells/mm^2 were obtained on the sample plates. The plates were then coated with sputtered silver and analyzed by MALDI-IM-MS.

Cell Culture for Monolayer Imaging

ITO-coated glass plates were dip-coated with poly-L-lysine followed by washing with H_2O (×5). The edges of the plates were marked with a hydrophobic marker to prevent overflow of the cell suspension. The plates were kept in DMEM medium until use. Control and SLOS human fibroblasts were maintained in DMEM supplemented with L-glutamine, 10% FBS, and penicillin/streptomycin at 37°C and 5% CO_2. The cells were trypsinized, counted, and re-suspended to a concentration of 1 million cells/mL in the above medium. Approximately 0.5 mL of the cell suspension (500,000 cells) was added onto the poly-L-lysine coated glass plates. The cell-covered plates were incubated at 37°C for 24 h before changing regular FBS containing medium to lipid-reduced FBS containing medium. The medium was changed every other day and the cells were grown for 6 d. The plates were then washed with 1× HBSS (×2) and H_2O (×2), and dried under air and subsequently under vacuum. Optimization of the sputtering duration on these plated non-trypsinized cells indicated a slightly shorter silver sputtering time of 300 s for highest analyte intensities in comparison with those found for the standards in the absence of the cellular matrix. Quantification of the ratios of 7-DHC/cholesterol from control and SLOS human fibroblast monolayers were obtained by surveying areas of ca. 2 mm^2 following silver deposition.

Ion Mobility-Mass Spectrometry Imaging and Optical Imaging of Human Fibroblast Monolayers

Areas of ca. 4.5×4.5 mm of the control and SLOS human fibroblast cell monolayers grown on ITO and poly-L-lysine-coated glass plates were imaged with MALDI-IM-MS after 300 s of silver sputter coating. The MALDI-IM-MS images were obtained using a laser diameter of 30 μm and data were collected with 2 μm oversampling (1000 shots of laser per pixel) [26]. This level of oversampling was chosen to demonstrate the ability to use IM-MS to image cultured cells at subcellular resolution and overlay these images with optical micrographs. Optical images of the same areas were taken on a Zeiss AXIO Observer.Z1 inverted microscope equipped with Hamamatsu Digital Camera C10600 Orca R^2 using AxioVision Rel. 4.7 program and subsequently co-registered with the MALDI-IM-MS images.

Results and Discussion

This research was motivated by two primary challenges in the determination of cholesterol, cholesterol precursors, and their quantitative ratios by MS techniques. First, attenuated sterol ionization using conventional MALDI protocols and chemical reactivity of the analytes in the sample preparation or the ionization process make it difficult to analyze the sterol species. This has been observed in spectra for cholesterol species in the literature, but

largely not described, because it was not the focus of those works [22].These phenomena are particularly salient in the present work because it confounds the analysis of cholesterol precursor species such as 7-DHC, a cholesterol precursor that was found to be the most reactive lipid molecule toward free radical oxidation [27]. We found that these effects can be largely mitigated by using gas-phase rather than liquid-phase silver deposition. Second, when analyzing these species directly from biological samples, such as human fibroblast cells in this work, extensive chemical noise in the low mass region makes it difficult to detect cholesterol and cholesterol precursors at biologically relevant concentrations. In part, these nominally isobaric species can be separated through the use of high resolution MS approaches (e.g., >30,000). Our approach is to separate the chemical noise from the analytes of interest through the use of ion-mobility (IM) MS.

Sputtered Silver MALDI-IM-MS Analysis of Cholesterol and 7-DHC Standards

Silver sputtering under the condition used in this report gives particle sizes of 10 to 25 nm as measured by scanning electron microscopy (Figure 1a). The particle size is about the same as the size of the colloidal AgNP (20 nm) used in this study and earlier reports [12].

Cholesterol and 7-DHC standards were spotted onto ITO-coated glass MALDI plates, coated by sputtered silver, and analyzed by MALDI-IM-MS. Silver coordination signals of $[\text{cholesterol+Ag}]^+$ (*m/z* 493 and 495) and $[\text{7-DHC+Ag}]^+$ (*m/z* 491 and 493) doublets were readily observed, and stand out distinctly from background signals in IM separation. Figure 1b shows the drift time versus *m/z* two-dimensional IM-MS spectrum of $[\text{cholesterol+Ag}]^+$, and Figure 1c and d show the typical MS spectra pre- and post-IM separation. The ability to select only $[\text{M+Ag}]^+$ as shown on Figure 1d allows strong isobaric noise contributors with different mobility to be completely eliminated. Indeed, the elimination of chemical noise leads to >500 times signal-to-noise (S/N) increase when assaying cholesterol at a concentration of 4 pmol/mm^2. The drift-time selection rule was established using cholesterol and 7-DHC standards and the same rule was applied to the studies on human fibroblast cells as discussed in sections below. In establishing this selection rule, it is assumed that any contribution from differences in cellular media or cell type to noise sources is minimal over the regions selected and the effect of that noise on the MS signal intensity of the analytes of interest is the same.

By varying the sputtering time while keeping other conditions the same, the highest signal intensity for both $[\text{cholesterol+Ag}]^+$ and $[\text{7-DHC+Ag}]^+$ was achieved with 600 s of silver sputtering for the sterol standards (Supplementary Figures S1 and S2). Cholesterol clearly responds better than 7-DHC in the sputtered silver MALDI-IM-MS. The response factor of 7-DHC relative to cholesterol was determined to be 1.26 and was used to estimate the ratios of these two sterols in in human fibroblasts (see below).

Comparison of Gas-Based Sputtered Silver and Liquid-Based Silver

In addition to sputtering, MALDI-IM-MS analysis of $[\text{cholesterol+Ag}]^+$ and $[\text{7-DHC+Ag}]^+$ was also achieved with $AgNO_3$ solution and colloidal AgNP. Solution silver deposition appears to give the lowest limit-of-detection (LOD) at ca. 0.5 pmol/mm^2, but large number of dehydrogenation peaks, $[\text{M+Ag-2H}]^+$, were observed for both $[\text{cholesterol+ Ag}]^+$ and [7-

DHC+Ag]$^+$ (Figure 2). It should be noted that this dehydrogenation phenomenon of cholesterol silver adducts was also observed previously by Nygren and co-workers using SIMS [21]. The formation of the dehydrogenation ions is potentially problematic when both cholesterol and 7-DHC are being assayed. For example, overestimation of the levels of 7-DHC and underestimation of the levels of cholesterol would be expected when analyzing control human fibroblasts because the low levels of 7-DHC and high levels of cholesterol in these cells. In comparison, silver sputtering, besides being a rapid and reproducible technique to deposit silver particles with controllable size, produced an LOD for cholesterol and 7-DHC standards similar to silver deposition by $AgNO_3$ solution. More importantly, dehydrogenation signals decreased with sputtered silver, which allows higher accuracy and reproducibility when measuring the ratios of 7-DHC/cholesterol. Colloidal AgNP did not produce significant dehydrogenation peaks, but the LOD is relatively high at ca. 5 pmol/mm^2, which is consistent with the value reported previously [12]. Interestingly, colloidal AgNP MALDI-IM-MS also led to the detection of peaks that are two mass units higher than the expected *m/z* values when analyzing 7-DHC standard (i.e., peaks with *m/z* of [7-DHC+Ag+2H]$^+$). A comparison of these three methods of silver application is summarized in Table 1.

We note that even though sputtered silver gave the least amount of dehydrogenation peaks, this process was not fully eliminated. In fact, as seen in Figure 2, the integrated relative signal (to the base peak) from dehydrogenation of the [7-DHC+^{107}Ag$^+$] adduct is more than four times that from dehydrogenation of the [cholesterol+^{107}Ag$^+$] adduct, suggesting the doubly unsaturated 7-DHC is more prone to oxidation (dehydrogenation) than cholesterol in the gas phase. This observation is consistent with the high oxidizability of 7-DHC in solution and liposome [27]. Indeed, 7-DHC was found to be the most reactive lipid molecule known to date in a free radical-mediated oxidation reaction in solution, a property that may be important to the understanding of its gas-phase behavior [27].

Analysis of Cholesterol and 7-DHC in Control and SLOS Human Fibroblasts

Control and SLOS human fibroblasts were grown in lipid-reduced medium for 6 d to allow de novo biosynthesis of cholesterol, which is necessary for the accumulation of 7-DHC in these cells [25]. To obtain the LOD of cholesterol in cells, the human fibroblast cells were trypsinized, suspended at different concentrations in PBS buffer, and then spotted on ITO-coated glass plates (leading to spots of 100, 1000, and 10,000 cells/mm^2) for assaying with sputtered Ag MALDI-IM-MS (Figure 3). We found that a minimum density of ca. 1000 cells/mm^2 was required to achieve a S/N ratio of 3 from the [cholesterol+Ag]$^+$ peaks in control and SLOS human fibroblasts. However, we want to point out a potentially important difference between trypsinized cells and the monolayer cells adhering to the surface of glass plates (non-trypsinized). Non-trypsinized cells are elongated on the plates and occupy large surface areas, whereas trypsinized cells are rounded up and present less surface area. Therefore, it is possible that the non-trypsinized monolayer cells will provide different figures-of-merit from the trypsinized cells in the MALDI process.

To extend our methodology to analyzing cholesterol and 7-DHC in cells in situ, we grew human fibroblast monolayer cells directly on poly-L-lysine-coated ITO glass plates for 6 d

in cholesterol-free medium. The cell density was estimated to be 1200–1300 cells/mm^2 based on the initial cell numbers (500,000 cells/plate) and the doubling time of these cell lines (72 h). The optimum sputtering time for achieving the greatest signal intensities when analyzing these monolayer cells was found to be 300 s (Supplementary Figure S3), although signal intensities for 600 and 900 s were only slightly reduced from 300 s. Using sputtered silver MALDI-IM-MS analysis, [cholesterol+Ag]$^+$ and [7-DHC+Ag]$^+$ signals are clearly observed in these monolayer cells (Figure 4). Utilizing these conditions, the 7-DHC/cholesterol ratio was evaluated, which is represented by the ratio of *m/z* 491 (specific for [7-DHC+^{107}Ag]$^+$) to 495 (specific for [cholesterol+^{109}Ag]$^+$), in SLOS human fibroblasts. This ratio was determined to be 0.54±0.16, whereas the same ratio was found to be 0.21±0.02 in control human fibroblasts. Furthermore, the ratio for control cells is likely to be overestimated because of the dehydrogenation ion (*m/z* 491) formed from the corresponding [cholesterol+Ag]$^+$ peak (*m/z* 493), as control cells are known to have detectable but low levels of 7-DHC [25]. On the other hand, the ratio for SLOS cells is likely to be underestimated because of the dehydrogenation of [7-DHC+^{107}Ag]$^+$ (*m/z* 491) and high level of 7-DHC in these cells. In support of this interpretation, we found that although 300 s of silver sputtering gave highest signal intensity in the cells tested, 100 s of sputtering led to less dehydrogenation of the silver adducts, yielding a 7-DHC/cholesterol ratio of 0.86±0.18 and 0.14±0.02 for the same SLOS and control fibroblast samples, respectively. This observation again suggested that the [7-DHC+Ag]$^+$ adducts are more prone to dehydrogenation in the gas phase than the [cholesterol+Ag]$^+$ adducts.

Imaging of Cholesterol, 7-DHC, and 7-DHC/Cholesterol in Control and SLOS Human Fibroblasts

Owing to the optical transparency of the ITO-coated glass plates, both optical and MS images on the monolayer cells for co-registration were obtained. The *m/z* of 491 and 495 were imaged using imaging IM-MS of both control and SLOS human fibroblasts (Figure 4), where increased levels of 7-DHC and decreased levels of cholesterol are observed in the SLOS versus control fibroblasts, respectively.

Co-registration of a representative pair of optical images with the imaging IM-MS image is shown in Figure 5a, and additional images of this type are presented in Supplementary Figures S4 and S5. From these images, the MS signal intensity is low or absent in regions of low cell density or gaps on the plate and the MS signal is high where the cell density increases. Although we are not claiming single cell detection because of the current instrument limitations (e.g., laser irradiation dimensions, minimum step, sensitivity, etc.), the spatial resolution of this sputter-coated silver approach may lead to single-cell MALDI-MS imaging of sterols in the future.

Images corresponding to the ratios of 7-DHC/cholesterol in control and SLOS human fibroblasts were also obtained from matched images. As illustrated in Figure 5b, in a cell-covered region, the 7-DHC/cholesterol ratios are distinctly larger in SLOS samples than in controls. This demonstrated the capability of this technique in obtaining the ratio of 7-DHC/cholesterol in a high-throughput fashion attributable to the requirement for minimum sample processing, and its potential application in diagnosing/assaying the severity of cholesterol

biosynthesis diseases, such as SLOS. The exceptional susceptibility of 7-DHC to oxidation, which leads to the formation of cytotoxic oxidative metabolites [28, 29], underscores the need for such rapid diagnostic methods as developed here [8, 9, 30, 31].

Conclusions

Here we demonstrated the application of gas-based sputtered-silver MALDI-IM-MS in profiling cholesterol and its biosynthetic precursor, 7-DHC, from spotted and plated cells, and in imaging IM-MS of plated cells. Using this approach, fibroblast cells from normal individuals and SLOS patients may be rapidly differentiated by assaying the levels of cholesterol and 7-DHC in small numbers of trypsinized or monolayer cells (1000 cells/mm^2). We also successfully imaged cholesterol, 7-DHC, and 7-DHC/cholesterol ratios in both control and SLOS human fibroblast cell monolayers that were grown directly on the glass sample plates. The MALDI-IM-MS approach allows high throughput profiling and imaging of cell culture assays in cases where it offers sufficient sensitivity of detection for the analytes. In contrast, LC approaches require additional multiple steps including lipid extraction, evaporation, and re-constitution of the extracts. The MALDI-IM-MS method can potentially be expanded to analyze or image other sterol precursors and olefins that share unconjugated double bond systems present in cholesterol and 7-DHC. The capability to image cholesterol precursors to cholesterol ratios directly on intact monolayer cells with minimum sample processing may provide a high-throughput screening assay for agents that alter cholesterol biosynthesis. Inhibition of cholesterol biosynthesis leads to detrimental accumulation of cholesterol precursors, but up-regulation of the expression of cholesterol biosynthesis enzymes, such as DHCR7, may provide an opportunity to develop new therapy for cholesterol biosynthesis disorders like SLOS.

Supplementary Material

Refer to Web version on PubMed Central for supplementary material.

Acknowledgments

The authors acknowledge the Vanderbilt Institute of Nanoscale Science and Engineering (VINSE) for use of the scanning electron microscope. We want to thank Dr. Aaron Bowman for the use of the Zeiss AXIO Observer.Z1 inverted microscope. This work was supported by Vanderbilt College of Arts and Science, Vanderbilt Institute of Chemical Biology, Vanderbilt Institute for Integrative Biosystems Research and Education, Vanderbilt Kennedy Center for Research on Human Development, NIH [K99HD073270 (L.X.), ES013125 and HD064727 (N.P.), UH2TR000491 (J.A.M.)], and the Defense Threat Reduction Agency (HDTRA1-09-1-00-13 (JAM).

References

1. Brown DA, London E. Functions of lipid rafts in biological membranes. Annu Rev Cell Dev Biol. 1998; 14:111–136. [PubMed: 9891780]
2. Korade Z, Kenworthy AK. Lipid rafts, cholesterol, and the brain. Neuropharmacology. 2008; 55:1265–1273. [PubMed: 18402986]
3. Dietschy JM, Turley SD. Cholesterol metabolism in the brain. Curr Opin Lipidol. 2001; 12:105–112. [PubMed: 11264981]
4. Porter JA, Young KE, Beachy PA. Cholesterol modification of Hedgehog signaling proteins in animal development. Science. 1996; 274:255–259. [PubMed: 8824192]

5. Porter FD, Herman GE. Malformation syndromes caused by disorders of cholesterol synthesis. J Lipid Res. 2011; 52:6–34. [PubMed: 20929975]

6. Brown MS, Goldstein JL. Lipoprotein metabolism in the macrophage: implications for cholesterol deposition in atherosclerosis. Annu Rev Biochem. 1983; 52:223–261. [PubMed: 6311077]

7. Carstea ED, Morris JA, Coleman KG, Loftus SK, Zhang D, Cummings C, Gu J, Rosenfeld MA, Pavan WJ, Krizman DB, Nagle J, Polymeropoulos MH, Sturley SL, Ioannou YA, Higgins ME, Comly M, Cooney A, Brown A, Kaneski CR, Blanchette-Mackie EJ, Dwyer NK, Neufeld EB, Chang TY, Liscum L, Strauss JF 3rd, Ohno K, Zeigler M, Carmi R, Sokol J, Markie D, O'Neill RR, van Diggelen OP, Elleder M, Patterson MC, Brady RO, Vanier MT, Pentchev PG, Tagle DA. Niemann-Pick C1 disease gene: homology to mediators of cholesterol homeostasis. Science. 1997; 277:228–231. [PubMed: 9211849]

8. de Sain-van der Velden MGM, Verrips A, Prinsen BH, de Barse M, Berger R, Visser G. Elevated cholesterol precursors other than cholestanol can also be a hallmark for CTX. J Inherit Metab Dis. 2008; 31(Suppl 2):387–393.

9. Payré B, de Medina P, Boubekeur N, Mhamdi L, Bertrand-Michel J, Tercé F, Fourquaux I, Goudounèche D, Record M, Poirot M, Silvente-Poirot S. Microsomal antiestrogen-binding site ligands induce growth control and differentiation of human breast cancer cells through the modulation of cholesterol metabolism. Mol Cancer Ther. 2008; 7:3707–3718. [PubMed: 19074846]

10. Bayer E, Gfrorer P, Rentel C. Coordination-ionspray-MS (CIS-MS), a universal detection and characterization method for direct coupling with separation techniques. Angew Chem Int Ed. 1999; 38:992–995.

11. Rentel C, Strohschein S, Albert K, Bayer E. Silver-plated vitamins: a method of detecting tocopherols and carotenoids in LC/ESI-MS coupling. Anal Chem. 1998; 70:4394–4400. [PubMed: 9796422]

12. Sherrod SD, Diaz AJ, Russell WK, Cremer PS, Russell DH. Silver nanoparticles as selective ionization probes for analysis of olefins by mass spectrometry. Anal Chem. 2008; 80:6796–6799. [PubMed: 18671412]

13. Perdian DC, Cha S, Oh J, Sakaguchi DS, Yeung ES, Lee YJ. In situ probing of cholesterol in astrocytes at the single-cell level using laser desorption ionization mass spectrometric imaging with colloidal silver. Rapid Commun Mass Spectrom. 2010; 24:1147–1154. [PubMed: 20301106]

14. Niziol J, Rode W, Laskowska B, Ruman T. Novel monoisotopic 109AgNPET for laser desorption/ionization mass spectrometry. Anal Chem. 2013; 85:1926–1931. [PubMed: 23320778]

15. Patti GJ, Shriver LP, Wassif CA, Woo HK, Uritboonthai W, Apon J, Manchester M, Porter FD, Siuzdak G. Nanostructure-initiator mass spectrometry (NIMS) imaging of brain cholesterol metabolites in Smith-Lemli-Opitz syndrome. Neuroscience. 2010; 170:858–864. [PubMed: 20670678]

16. Maréchal N, Quesnel E, Pauleau Y. Silver thin films deposited by magnetron sputtering. Thin Solid Films. 1994; 241:34–38.

17. Altelaar AF, Klinkert I, Jalink K, de Lange RP, Adan RA, Heeren RM, Piersma SR. Gold-enhanced biomolecular surface imaging of cells and tissue by SIMS and MALDI mass spectrometry. Anal Chem. 2006; 78:734–742. [PubMed: 16448046]

18. Sjovall P, Lausmaa J, Nygren H, Carlsson L, Malmberg P. Imaging of membrane lipids in single cells by imprint-imaging time-of-flight secondary ion mass spectrometry. Anal Chem. 2003; 75:3429–3434. [PubMed: 14570193]

19. Nygren H, Malmberg P. Silver deposition on freeze-dried cells allows subcellular localization of cholesterol with imaging TOF-SIMS. J Microsc. 2004; 215:156–161. [PubMed: 15315502]

20. Nygren H, Johansson BR, Malmberg P. Bioimaging TOF-SIMS of tissues by gold ion bombardment of a silver-coated thin section. Microsc Res Tech. 2004; 65:282–286. [PubMed: 15662659]

21. Nygren H, Malmberg P, Kriegeskotte C, Arlinghaus HF. Bioimaging TOF-SIMS: localization of cholesterol in rat kidney sections. FEBS Lett. 2004; 566:291–293. [PubMed: 15147911]

22. Dufresne M, Thomas A, Breault-Turcot J, Masson JF, Chaurand P. Silver-assisted laser desorption ionization for high spatial resolution imaging mass spectrometry of olefins from thin tissue sections. Anal Chem. 2013; 85:3318–3324. [PubMed: 23425078]

23. Tanaka K, Waki H, Ido Y, Akita S, Yoshida Y, Yoshida T, Matsuo T. Protein and polymer analyses up to *m/z* 100,000 by laser ionization time-of-flight mass spectrometry. Rapid Commun Mass Spectrom. 1988; 2:151–153.

24. McLean JA, Stumpo KA, Russell DH. Size-selected (2–10 nm) gold nanoparticles for matrix assisted laser desorption ionization of peptides. J Am Chem Soc. 2005; 127:5304–5305. [PubMed: 15826152]

25. Xu L, Korade Z, Rosado DA, Liu W, Lamberson CA, Porter NA. Metabolism of oxysterols derived from nonenzymatic oxidation of 7-dehydrocholesterol in cells. J Lipid Res. 2011; 52:1222–1233. [PubMed: 21402677]

26. Jurchen JC, Rubakhin SS, Sweedler JV. MALDI-MS imaging of features smaller than the size of the laser beam. J Am Soc Mass Spectrom. 2005; 16:1654–1659. [PubMed: 16095912]

27. Xu L, Davis TA, Porter NA. Rate constants for peroxidation of polyunsaturated fatty acids and sterols in solution and in liposomes. J Am Chem Soc. 2009; 131:13037–13044. [PubMed: 19705847]

28. Xu L, Korade Z, Porter NA. Oxysterols from free radical chain oxidation of 7-dehydrocholesterol: product and mechanistic studies. J Am Chem Soc. 2010; 132:2222–2232. [PubMed: 20121089]

29. Korade Z, Xu L, Shelton R, Porter NA. Biological activities of 7-dehydrocholesterol-derived oxysterols: implications for Smith-Lemli-Opitz syndrome. J Lipid Res. 2010; 51:3259–3269. [PubMed: 20702862]

30. Martanova H, Krepelova A, Baxova A, Hansikova H, Cansky Z, Kvapil M, Gregor V, Magner M, Zeman J. X-linked dominant chondrodysplasia punctata (CDPX2): multisystemic impact of the defect in cholesterol biosynthesis. Prague Med Rep. 2007; 108:263–269.

31. Wolthers BG, Walrecht HT, van der Molen JC, Nagel GT, Van Doormaal JJ, Wijnandts PN. Use of determinations of 7-lathosterol (5 alpha-cholest-7-en-3 beta-ol) and other cholesterol precursors in serum in the study and treatment of disturbances of sterol metabolism, particularly cerebrotendinous xanthomatosis. J Lipid Res. 1991; 32:603–612. [PubMed: 1856606]

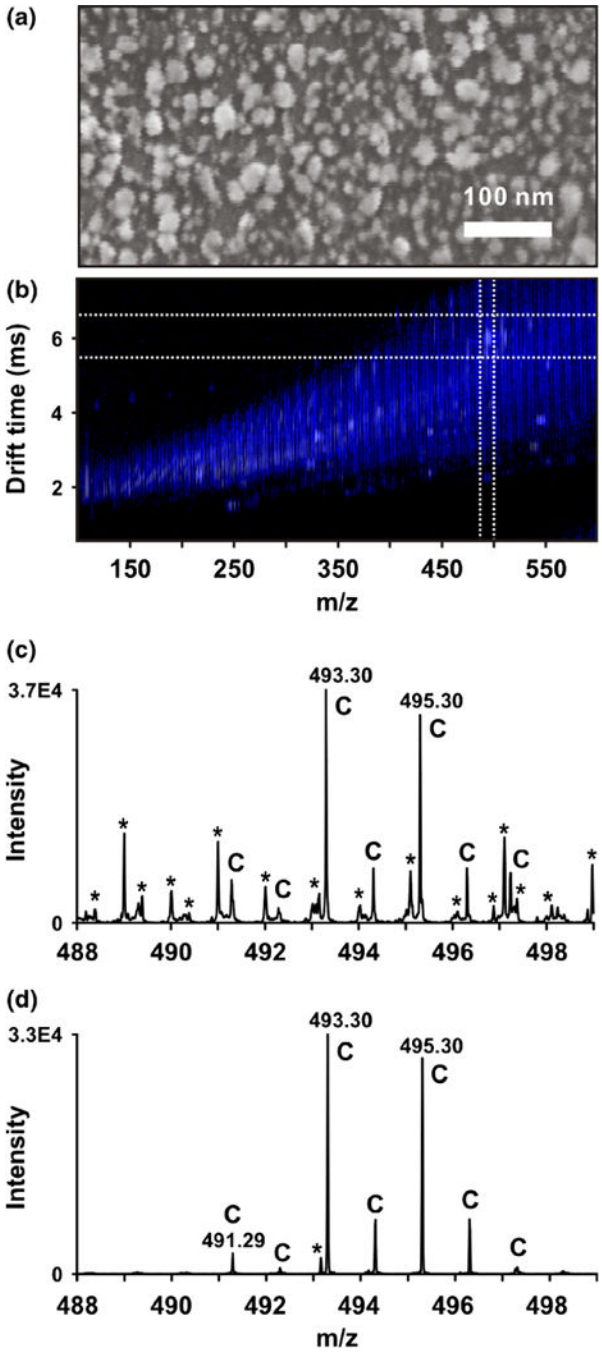

Figure 1.

Sputtered silver MALDI-IM-MS analysis of cholesterol standard on an ITO-coated glass MALDI plate. (**a**) Scanning electron microscopy image of nanoparticles formed from sputtered silver. Average particle size is approximately 20 nm. (**b**) Two-dimensional IM-MS spectrum of cholesterol standard. Cholesterol-silver adducts are highlighted in the white box. (**c**) Mass spectrum of cholesterol-silver adducts without IM separation (i.e., integrated across all drift times between *m/z* 488 and 498). Peaks corresponding to cholesterol and related species are labeled “C” and chemical noise is labeled with *asterisks* *. (**d**) Mass

spectrum of cholesterol-silver adducts over the ion mobility drift time region indicated by dashed lines in (**a**). Significant S/N improvement of cholesterol is achieved via exclusion of chemical noise

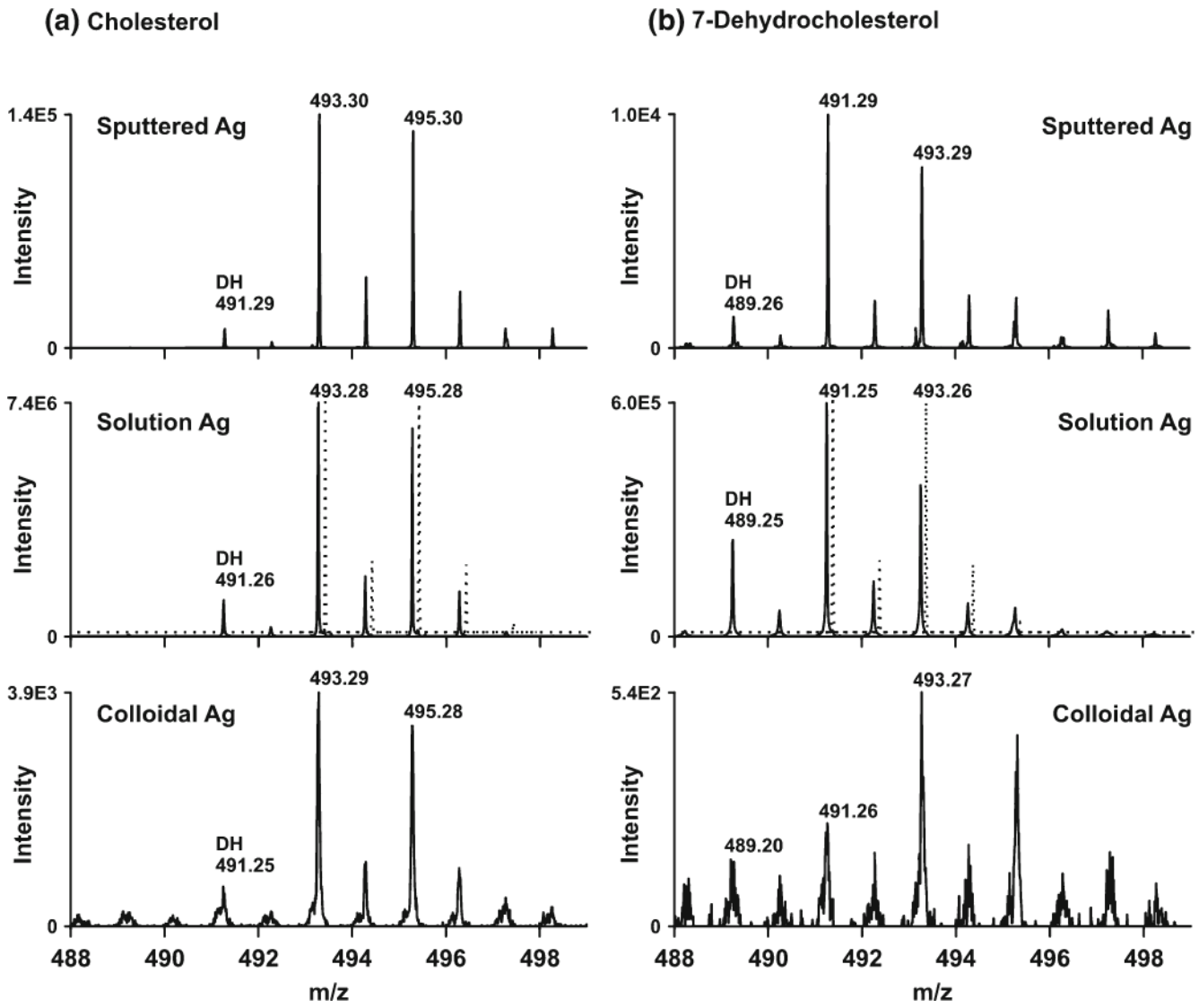

Figure 2.

Comparison of sputtered Ag, solution $AgNO_3$, and colloidal AgNP in the MALDI-IM-MS analysis of (**a**) cholesterol standard at 39 pmol/mm^2 and (**b**) 7-DHC standard at 36 pmol/mm^2. The theoretical distribution of [cholesterol+Ag^+] and [7-DHC+Ag^+] species is indicated by the offset dashed-lines in the middle panels for reference

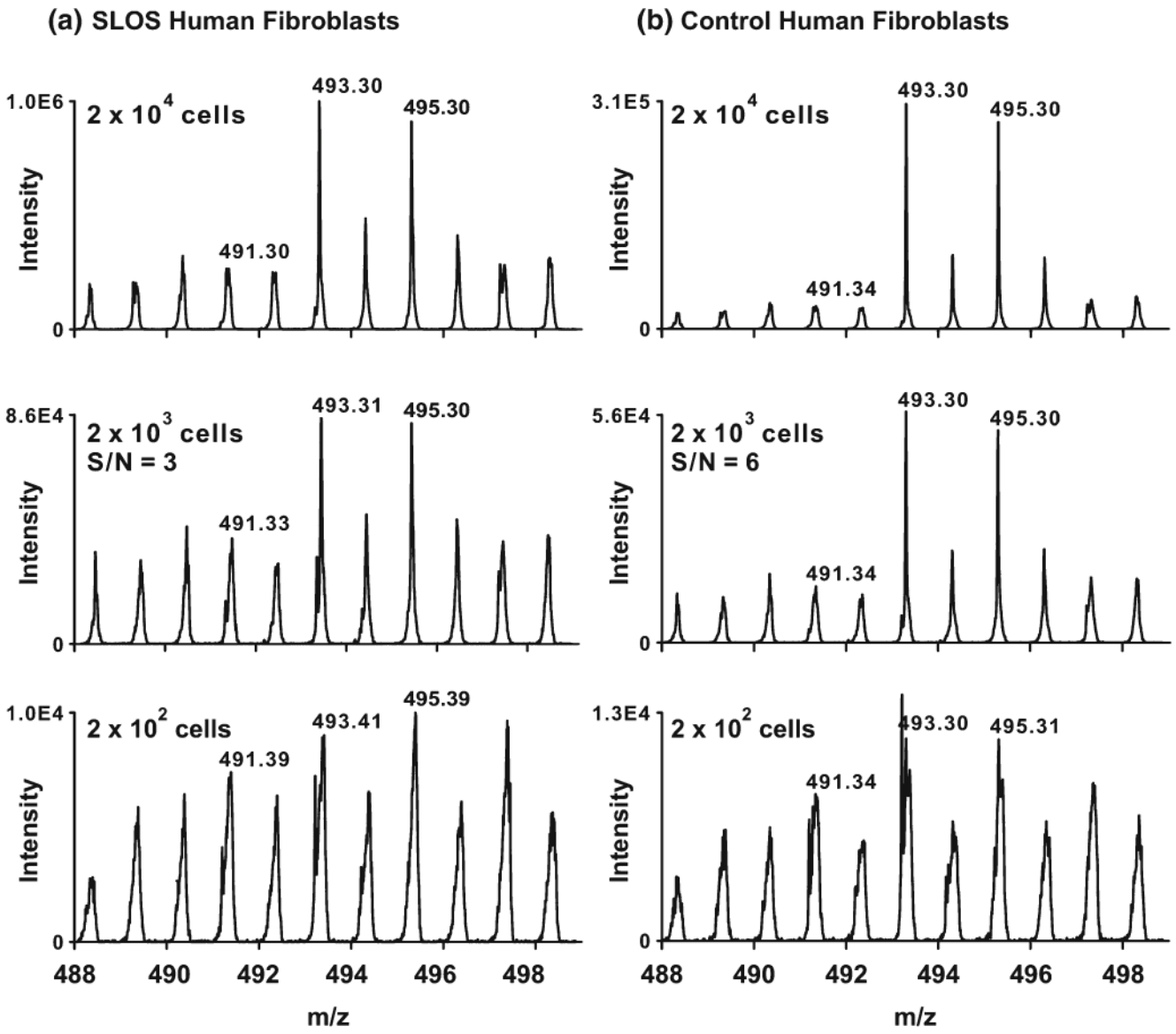

Figure 3.

Analysis of sterols in SLOS (**a**) and control (**b**) human fibroblasts. Cells were trypsinized and different concentrations of the cell suspension were spotted on target. S/N ratios were estimated by integrating the spectrum and dividing the area corresponding to *m/z* 493 by *m/z* 488 (corresponding to chemical and instrumental noise)

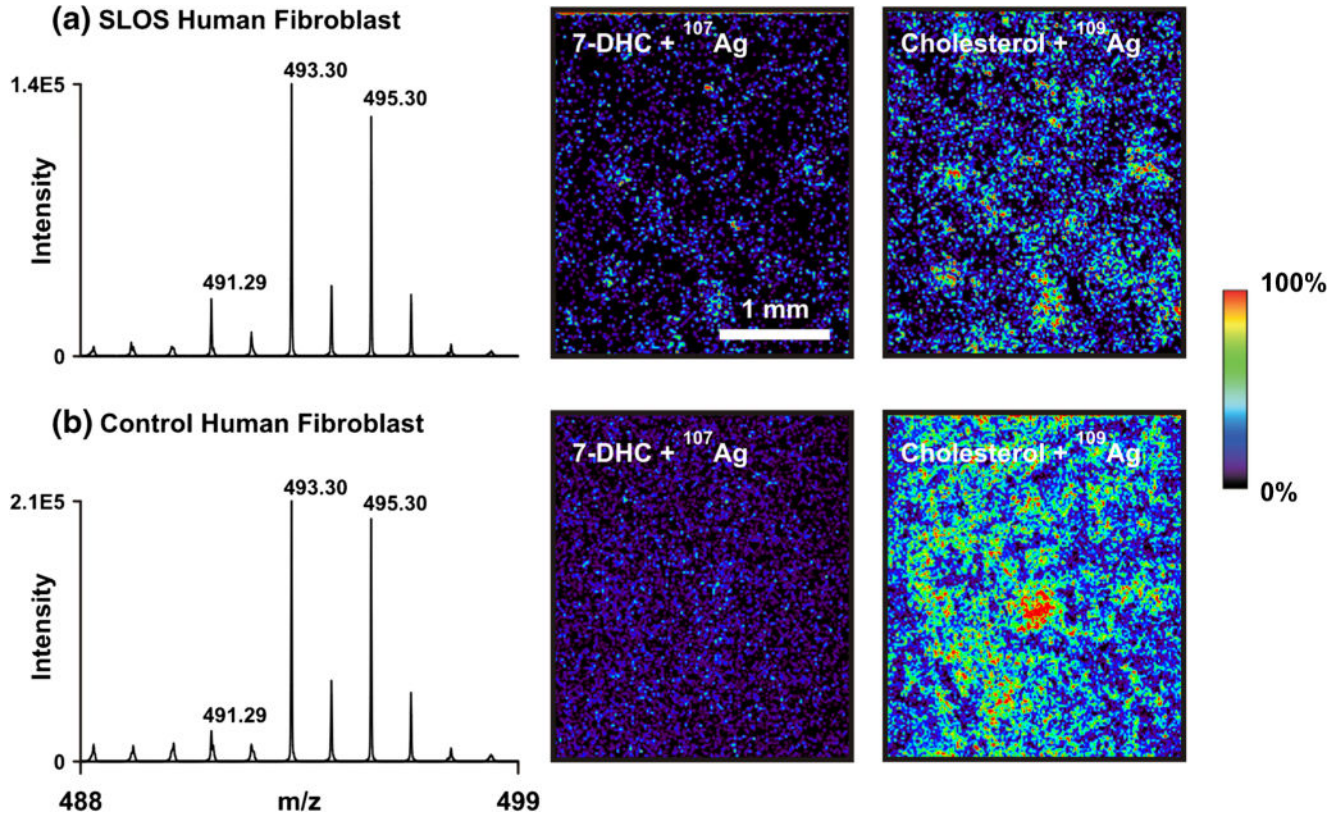

Figure 4.

Imaging IM-MS of cholesterol and 7-DHC in SLOS (**a**) and control (**b**) human fibroblasts grown directly on ITO-coated plates. The *m/z* of 491 is specific for $[7\text{-DHC}+^{107}\text{Ag}]^+$ and 495 is specific for $[\text{cholesterol}-^{109}\text{Ag}]^+$

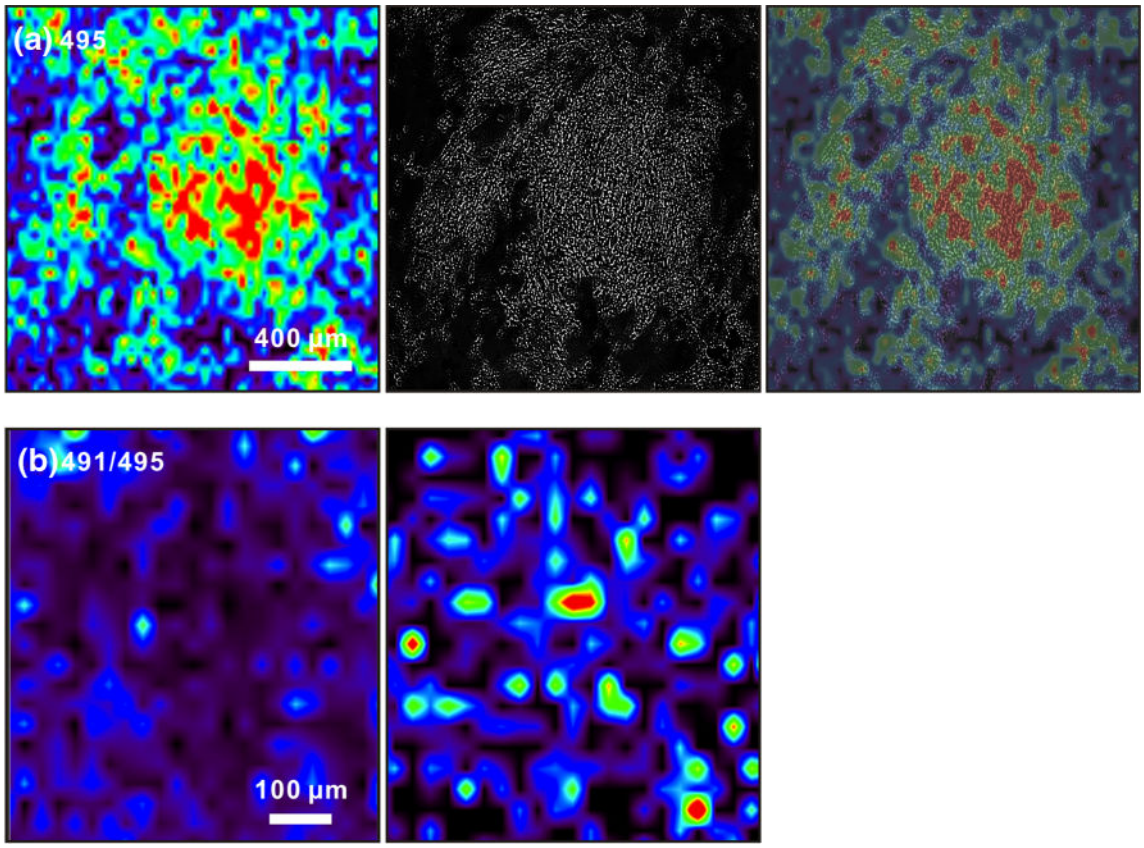

Figure 5.

(**a**) Imaging IM-MS of cholesterol at *m/z* 495 (left), an optical image of the field of cells (center), and an overlay of both images (right) illustrating co-registration of the optical and *m/z* images. (**b**) Imaging IM-MS of the ratio of $[7\text{-DHC}+^{107}\text{Ag}]^+/[\text{cholesterol}+^{109}\text{Ag}]^+$ (*m/z* 491/495) in control (*left*) and SLOS (*right*) human fibroblast cells. The ratio of these two ion images is obtained through ratioing the signal intensities of each specific *m/z* at each pixel coordinate

Table 1

Comparison of the Three Silver Coating Methods Tested in this Study

Silver source	Particle size (nm)	Reproducibility of application	Analyte diffusion	Limit-of-detection (pmol/mm^2)	Dehydrogenation of parent ions (%)[a]	
					[Cholesterol+Ag^+]	[7-DHC+Ag^+]
Sputtered Ag	10–25	Good	No	0.5	8	13
Solution Ag ($AgNO_3$)	Unknown	Poor	Yes	0.5	15	41
Colloidal Ag (NP)	20	Poor	Yes	5	17	_[b]

[a] Height percentage of the dehydration ions relative to the base peak

[b] Signal-to-noise is too low for accurate determination of the dehydrogenation percentage